Analytical Methods

PAPER

Cite this: *Anal. Methods*, 2016, **8**, 7910

Direct detection of tryptophan for rapid diagnosis of cancer cell metastasis competence by an ultra-sensitive and highly selective electrochemical biosensor†

M. R. Majidi,*[a] P. Karami,[ab] M. Johari-Ahar[c] and Y. Omidi*[b]

The detection of L-tryptophan (Trp) in the extracellular matrix (ECM) of solid tumors is important, particularly in metastatic tumors, which catabolize Trp to kynurenine to escape from host immune system-mediated recognition. The presence of a co-existing amino acid such as L-tyrosine (Tyr) in the ECM routinely interferes with the detection of Trp. The current study demonstrates the development of aptamer-assisted ultra-sensitive and label free biosensor (aptasensor) based on the constant current-potentiometric striping analysis (CC-PSA) technique used for quantitative Trp analysis. To prepare the aptasensor, a gold electrode was first decorated with carboxylated multiwall carbon nanotubes (MWCNTs) and then armed with Trp aptamer molecules (Apt). The engineered aptasensor was characterized electrochemically by cyclic voltammetry (CV), linear sweep voltammetry (LSV), and CC-PSA. For this biosensor, the limit of detection (LOD) was found to be 6.4×10^{-11} M (S/N = 3) and two linear detection ranges (*i.e.* 1.0×10^{-10} to 1.0×10^{-5} and 1.0×10^{-5} to 3.0×10^{-4} M) were observed in the calibration graph. For proof-of-technology, the aptasensor was used for the detection of Trp in biological samples such as cow's milk and human blood serum, saliva, and urine samples. Taking a good facet of the proposed aptasensor into account, it was implemented for the detection of the Trp consumption rate in various human cancer cell lines such as HepG2 (hepatocarcinoma), 1321NI (astrocytoma), Calu-6 (lung carcinoma), NCI-H1299 (lung carcinoma), and HT29 (colorectal carcinoma).

Received 24th July 2016
Accepted 10th October 2016

DOI: 10.1039/c6ay02103d

www.rsc.org/methods

Introduction

L-Tryptophan (Trp) is an essential amino acid that functions key roles in maintaining health and preventing disease. The detection of this amino acid in the extra cellular matrix (ECM) is of great importance in basic and clinical studies, particularly in the field of neuroscience and oncology.[1–4]

Several studies revealed that metastatic cancer cells increase their Trp metabolism through the induction of enzymes indoleamine 2,3-dioxygenase (IDO) and tryptophan-2,3-dioxygenase (TDO) to[5,6] suppress immunosurveillance and progression of malignancies.[7–10] Primary cancer starts as a local disease, but it can metastasize to the lymph nodes and distant organs. When spreading in the body, cancer no longer is primary, but its metastases at distant sites are the main cause of death. In recent years, prognostic markers are available to identify patients who are at the highest risk of developing metastases, which might enable oncologists to begin tailoring treatment strategies to individual patients. Measurements of the Trp consumption rate can be indicative of enzymes IDO and TDO activities and therefore, the degree of cancer cell metastasis.[11]

In the last two decades, some analytical methods have been developed for the determination of Trp.[12–16] Because the majority of these methods are mostly based on high performance liquid chromatography (HPLC), fluorometry, capillary electrophoresis (CE) and chemiluminescence techniques and are associated with some drawbacks, such as laborious, time consuming and costly procedures,[17–24] the development of fast, selective and cost-effective tools such as sensors/biosensors appears to be more in favor of basic and clinical studies. Biosensors represent simplicity, low expense, and possibility of miniaturization.

Of the various biosensors used in bioprocess monitoring, electrochemical biosensors, particularly potentiometric stripping analysis (PSA)-based sensors/biosensors in contrast to voltammetry methods, usually represent lower background

[a]*Department of Analytical Chemistry, Faculty of Chemistry, University of Tabriz, Tabriz, Iran. E-mail: majidi@tabrizu.ac.ir; Fax: +98 41 33340191; Tel: +98 41 33393111*

[b]*Research Center for Pharmaceutical Nanotechnology, Faculty of Pharmacy, Tabriz University of Medical Sciences, Tabriz, Iran. E-mail: yomidi@tbzmed.ac.ir; Fax: +98 41 33367929; Tel: +98 41 33367914*

[c]*Department of Medicinal Chemistry, School of Pharmacy, Ardabil University of Medical Sciences (ArUMS), Ardabil, Iran*

† Electronic supplementary information (ESI) available. See DOI: 10.1039/c6ay02103d

interferences that arise from the complex nature of biological media.[25–27]

Aptamer (Apt)-based electrochemical biosensors (the so-called aptasensors) have recently shown great promise for the selective and sensitive detection of biological targets. Aptamers,[28,29] which are synthetic DNA or RNA sequences, compared to antibodies (Abs) and other bio-recognition elements (*e.g.*, peptides) have shown comparable affinity but higher stability in bio-analytical assays.[30–32]

In this study, we demonstrate the development of ultra-sensitive and label free aptasensor for the rapid screening of Trp in biological samples and for the quantitative analysis of Trp consumption rate as a prognostic marker of metastasis in a number of cancer cell lines.

Materials and methods

Chemicals

Trp-specific RNA Apt (Trp-Apt) with sequence of 5′GGGAUCCUAAGCGACGAAGUUGAGGACCGGUACGGCCGCC-ACUCAGUAUCUACGCAUCGGA3′, which was previously reported by Majerfeld *et al.*[33] through systematic evolution of ligands by exponential enrichment (SELEX), was purchased from Bioneer Co., (Daejeon, Republic of Korea).

Trp, $K_4[Fe(CN)_6]$, $K_3[Fe(CN)_6]$, K_2HPO_4, KH_2PO_4, and trichloroacetic acid (TCA) were purchased from Merck Co., (Darmstadt, Germany). Ascorbic acid (AA), uric acid (UA), dopamine (DA), glucose, bovine serum albumin (BSA), tris(2,2′-bipyridine)ruthenium(II), amino acids for interference study, ethidium bromide (EthBr) for aptamer staining and carboxylated multiwall carbon nanotube (purity > 80%, average diameter 9.5 nm, length ~ 1.5 μm, COOH content > 8.00 wt%) were obtained from Sigma-Aldrich (Taufkirchen, Germany). Diethylpyrocarbonate (DEPC) water, used for preparation of aptamer solution, was prepared from Sinagen Co. (Tehran, Iran). The human cell lines (HepG2, 1321NI, Calu-6, NCI-H1299 and HT29) were obtained from Pasture Institute (Tehran, Iran). DMEM (Dulbecco's modified Eagle's medium) media component was purchased from Gibco (Invitrogen, Thermo Fisher Scientific, Erembodegem, Belgium). All chemicals were of analytical grade and used as received without any further purification. All solutions were prepared using deionized water (DI-water).

Apparatus

All electrochemical analysis was performed on an AutoLab PGSTAT30 Potentiostat/Galvanostat (Eco-Chemie, Utrecht; Netherland) using the GPES 4.7 software. A bare gold electrode (ϕ = 3 mm Metrohm Co., Schiedam, Netherlands) as the working electrode, a platinum wire as the counter electrode and Hg_2Cl_2/Hg (3 M KCl) as the reference electrode were utilized in the conventional three-electrode system.

Preparation of MWCNT-modified Au electrode

Gold electrodes (AuE) were successively polished by slurry alumina (0.05, 0.3 and 1.0 μm) and then by a polishing cloth for 2 min. Afterwards, the electrode was rinsed with DI-water and cleaned ultrasonically in a 1 : 1 mixture of ethanol : distilled water for 5 min. Following this step, the electrodes were immersed in piranha solution (3 : 1, sulphuric acid : hydrogen peroxide) for 10 min and then rinsed through a mixture of ethanol and DI-water (1 : 1 v/v) for the removal of residual particles from the electrodes surface.

In order to prepare carboxylated-multiwall carbon nanotube (MWCNT)-modified AuE (MWCNT-AuE), 5.0 mg of MWCNT was dispersed into 5.0 mL of DI-water and homogenized by Sonopuls HD 3200 (Bandelin Electronic, Berlin, Germany) for 10 min. A homogenous suspension of MWCNT was obtained at a power level of 25 W. Finally, six μL of the MWCNT suspension (1 mg mL^{-1}) was placed onto the cleaned electrodes uniformly and the solvent was allowed to be evaporated at 60 °C. This process was repeated twice to obtain a stable and uniform layer of MWCNT on the electrodes.

Deposition of Trp-specific Apt on the MWCNT-AuE (Apt–MWCNT-AuE)

Aptamer solution (1 μM) was prepared by adding lyophilized Apt into 1% DEPC solution in a micro tube container. Five μL of the prepared Apt solution was placed on MWCNT-AuE and dried at 60 °C for 30 min. In order to block the non-specific adsorption, the prepared electrodes were immersed in 1% BSA solution for 1 h, dried at 40 °C for 3 h, and finally stored at cool (8 °C) and dry place. In order to obtain stable and reproducible results, before each measurement with Apt–MWCNT-AuE, it was immersed in phosphate buffer solution (PBS, 0.01 M, pH 7.0) at 60 °C for 15 min. Scheme 1 represents the process of electrode preparation as well as electrochemical reactions being proposed mechanistically.

Fluorescence staining of deposited Apt on Apt–MWCNT-AuE

Ethidium bromide (EtBr), the small molecule intercalating the fluorescent dye that can stain single stranded ribonucleic acid (RNA) or deoxyribonucleic acid (DNA), was used for staining single Apt molecules deposited on MWCNT-AuE. After staining, Apt–MWCNT-AuE was washed with a PBS solution then visualized under UV light irradiation (254 nm) using UV cabinet (Taba Teb Co, Tehran, Iran).

Cancer cell culture and Trp rate determination

The human cancer cell lines were cultured in 6-well plates supplemented with DMEM containing 10% FBS, penicillin G (100 U mL^{-1}) and streptomycin (100 μg mL^{-1}) at 37 °C and 5% CO_2. The seeding density was 1.0×10^5 cells per well. Using Apt–MWCNT-AuE, the pattern of Trp consumption was studied through the sampling of supernatants analyzed immediately, and 1, 2 and 3 days of post-culture.

Conducting CC-PSA for determination of Trp

All electrochemical measurements were carried out in ambient conditions: 25 °C and relative humidity of 40%. A series of Trp solutions with standard concentrations ranging from 0.0 to

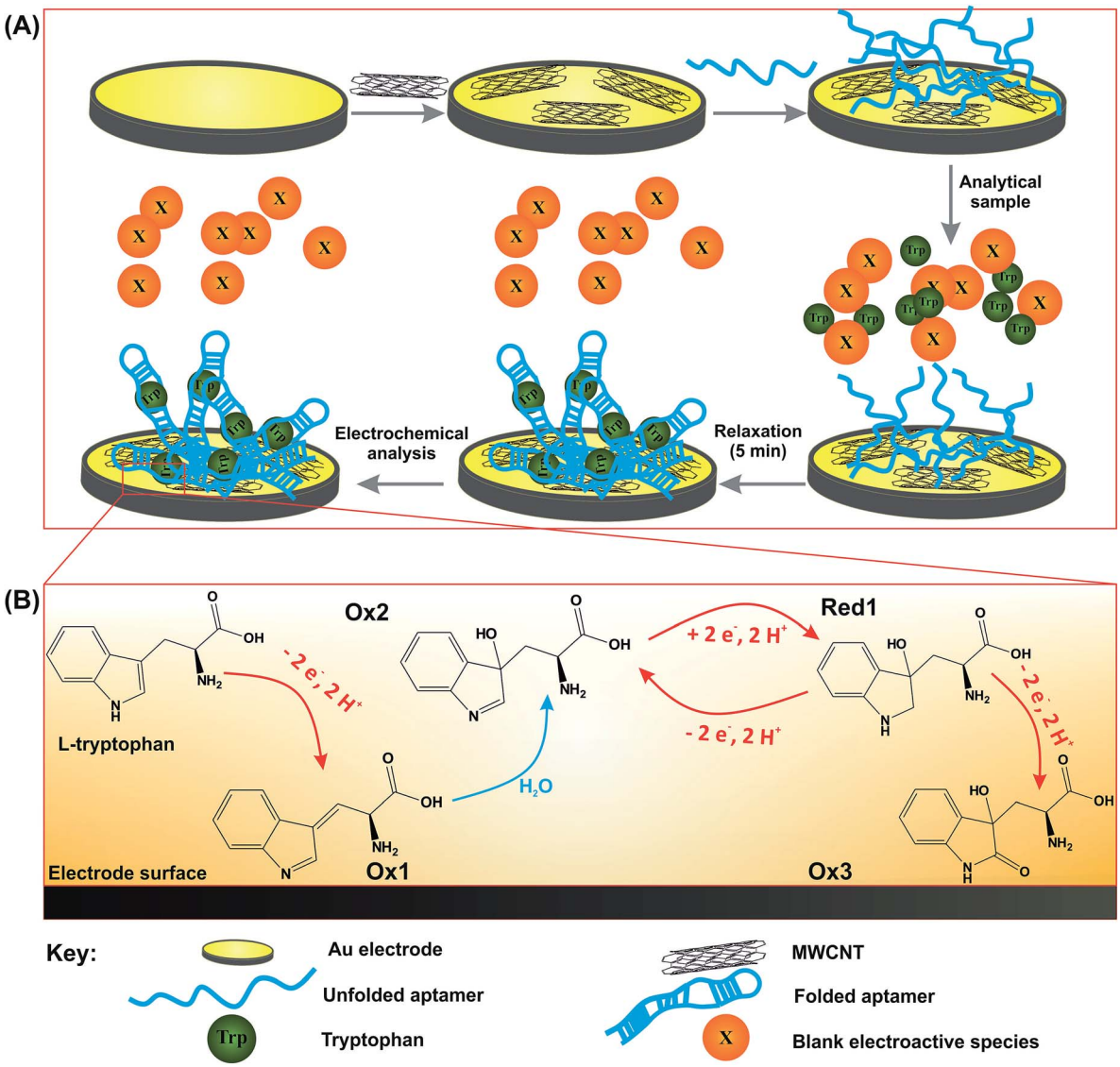

Scheme 1 (A) Preparation of Apt–MWCNT-AuE (aptasensor). (B) Proposed electrochemical reactions at the surface of the developed Trp aptasensor. Tryptophan: 2-amino-3-(1*H*-indol-3-yl)propanoic acid, Ox_1: 2-amino-3-(indolenine-3-ylene)propionic acid, Ox_2: 2-amino-3-(3-hydroxy-indolenine-3-yl)propionic acid, red_1: 2-amino-3-(3-hydroxy-1*H*-indoline-3-yl)propionic acid, Ox_3: 2-amino-3-(3-hydroxy,2-oxo-1*H*-indoline-3-yl)propionic acid.

300.0 μM was prepared in PBS (0.01 M, pH 7.0). For the completion of the folding process, Apt–MWCNT-AuEs were introduced to standard Trp solutions for 5 min and then analyzed by CC-PSA. The conditions in which CC-PSA measurements were performed included applying −0.2 V of conditional potential (E_c) for 10 s as a pre-treatment step and then recording the electrochemical signals in the range of 0.0 to +0.9 (V), obtained by applying a constant current (i_s) of +5 μA.

Analysis of Trp in biological/clinical samples

The potential basic and clinical applicability of the developed aptasensor was tested for the determination Trp in cow's milk as well as human urine, saliva and blood serum samples obtained from healthy volunteers. The results of the aptasensor were compared with those of high performance liquid chromatography (HPLC) analysis. The samples were diluted by 0.01 M PBS (pH 7.0) before analysis; urine and milk were diluted 10-fold, whereas saliva and blood serum samples were diluted 2-fold.

HPLC analysis

HPLC analyses were carried out according to the previously published method[34] using an Agilent 1100 system equipped with a fluorescence detector (Santa Clara, CA, United States). The chromatographic column used was Megres C18 (250 mm, 4.6 mm, 5 mm), Hanbon Sci. Tech. Co. (Jiangsu, China). The fluorescence signals were recorded at the optimal excitation (ex) and emission (em) wavelength of Trp (ex: 285 nm, em: 353 nm). In the sample preparation for the determination of free Trp before HPLC analyses, proteins in real samples (blood serum,

milk, and urine) were precipitated by the addition of 30% $HClO_4$. The samples then were vortexed for 10 s and centrifuged at 12 000*g* for 10 min. Saliva (one sample per each person) was collected into a beaker for 5 minutes during the day (10:00–11:00) and the saliva (0.1 mL) sample was mixed with 0.1 mL of 10% TCA. After centrifugation for 5 minutes at 21 000*g* at 4 °C, the deproteinized supernatant was collected and stored at −30 °C.[43] Subsequently, 10 μL of the supernatant was injected into the column, which was eluted with methanol–acetonitrile (1 : 1 v/v) with a flow rate of 0.8 mL min^{-1} at 25 °C.

Live subject statement

The authors state that all experiments were performed in compliance with the relevant laws and institutional guideline of National Committee of Ethics for Biomedical Research in Iranian Ministry of Health and Education. The authors also state that informed consent was obtained for any experimentation with human subjects and Committee of Ethics in Tabriz University of Medical Sciences, Iran, approved the experiments is committed to the protection and safety of human subjects involved in research.

Results and discussion

Characterization of the prepared electrodes

Cyclic voltammetry (CV) analysis. In the presence of Trp, the electro-catalytic characteristics of bare AuE, MWCNT-AuE, and Apt–MWCNT-AuE were identified by CV analyses at potentials lower than 1.0 V. Potentials greater than 1.0 V had destructive impacts on the secondary structure of the Apt molecules,[35,36] which is due mainly to the oxidation of guanine bases in the Apt structure.

Using the MWCNT-AuE, oxidation and reduction peaks of Trp were more clearly observed at 0.75 and 0.13 V, respectively (Fig. 1, panel (B), curve (b)). In the second CV scan, a couple of new oxidation peaks, corresponding to the oxidation of reduced byproducts produced in the first scan, appeared at 0.27 and 0.46 V, which were undetectable using bare AuE.

Fig. 1 (panels (A–C)) represents the CV spectra of the bare AuE, MWCNT-AuE and Apt–MWCNT-AuE in the presence (100 μM) and absence of Trp. As shown in Fig. 1 (panel (A)), the bare AuE, MWCNT-AuE Apt–MWCNT-AuE represented no significant electrochemical activity in the absence of Trp when added into the media; Trp could produce a faint signal using the bare AuE at the potential of 0.8 V (Fig. 1, panel (B), curve (a)).

It appears that Trp first is oxidized to Ox_1 (2-amino-3-(indolenine-3-ylene)propionic acid) that can easily react with H_2O molecules to produce Ox_2 (2-amino-3-(3-hydroxy-indolenine-3-yl)propionic acid)—highlighted in Scheme 1 (panel (B)). In the next step, Ox_2 is reduced to red_1 (2-amino-3-(3-hydroxy-1*H*-indoline-3-yl)propionic acid), following the first CV cycle. Subsequently, the produced red_1 is oxidized to Ox_2 and Ox_3 (2-amino-3-(3-hydroxy,2-oxo-1*H*-indoline-3-yl)propionic acid)[37,38] in the second CV cycle.

However, modification with MWCNT led to the amplification and resolution enhancement of the electrochemical peaks.

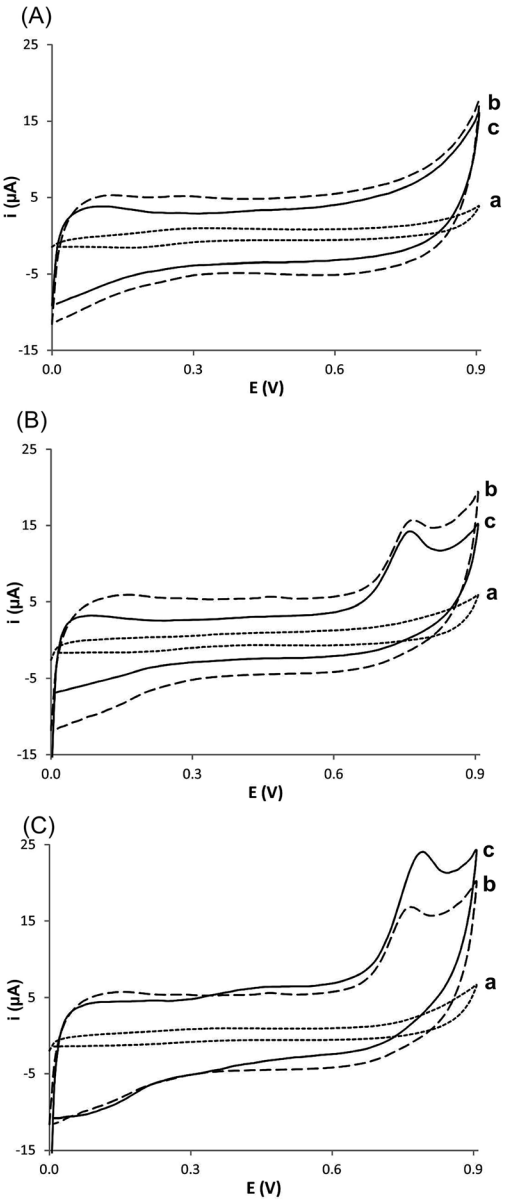

Fig. 1 CV analyses of (a) the bare AuE, (b) MWCNT-AuE, and (c) Apt–MWCNT-AuE obtained in the (A) absence and (B and C) presence of Trp, immediately after the addition of 100 μM Trp (B), and 5 min after post incubation with the Trp solution (100 μM) (C) at the scan rate of 0.1 V s^{-1}.

Using Apt–MWCNT-AuE, Trp oxidation and reduction peaks were observed at 0.80 V and 0.09 V (Fig. 1, panel (B), curve (c)); in the second CV scan, reduction peaks of byproducts formed at the first scan appeared at 0.13 V and 0.41 V.

Apt–MWCNT-AuE represented significant enhancement in the Trp oxidation peak when incubated with Trp for 5 min (Fig. 1, panel (C), curve (b)). It appears that the folding of Apt molecules deposited could concentrate Trp in close proximity with MWCNT at the electrode surface. In contrast, the signals from MWCNT-AuE were higher than that of Apt–MWCNT-AuE when a 5 min folding time was not allocated to Apt–MWCNT-AuE. Therefore, the dielectric effect of Apt molecules present on the electrode reduced the conductivity (Fig. 1, panel (C), curve

(c)), representing the crucial impact of folded Apt molecules in the signals transduction and amplification.

CC-PSA study

As represented in Fig. 2 (panel (A), curve (b)), CC-PSA signals of Trp oxidation are efficiently enhanced by MWCNT. In addition, unspecific signals from tyrosine oxidation are amplified using MWCNT and can interfere with the detection of Trp. Therefore, Apt–MWCNT-AuE was used for the analysis of Trp. This electrode sensed very faint signals of Trp oxidation when immersed in a Trp solution for 10 seconds and immediately analyzed without applying the incubation time (Fig. 2, panel (A), curve (c)). Interestingly, when incubated with Trp for 5 min, this electrode could detect the amplified signals of Trp oxidation at +0.74 V (Fig. 2, panel (B), curve (c)).

All this evidence demonstrates that Trp Apt molecules at the electrode surface can capture the Trp molecules, leading to the enhancement of the Trp signals. Altogether, Apt–MWCNT-AuE, benefiting from the outstanding electrical features of MWCNT and efficient pre-concentrating effects of Apt molecules, shows superiority to the MWCNT-AuE.

Determination of the surface area of the electrodes

The active surface area of the electrode usually increases with deposition of nanoparticles (NPs) on the electrode surface. Since the active sites available for the electrochemical reaction(s) can significantly increase with increasing active surface area of the modified electrodes, electrochemical signals are amplified effectively. As shown in Fig. S1 (see ESI†), the calculated values for the real surface area of AuE, MWCNT-AuE and Apt–MWCNT-AuE were found to be 0.103, 0.263 and 0.178 cm^2. These results confirm that the modification of the bare AuE with MWCNT extends the active surface area significantly.

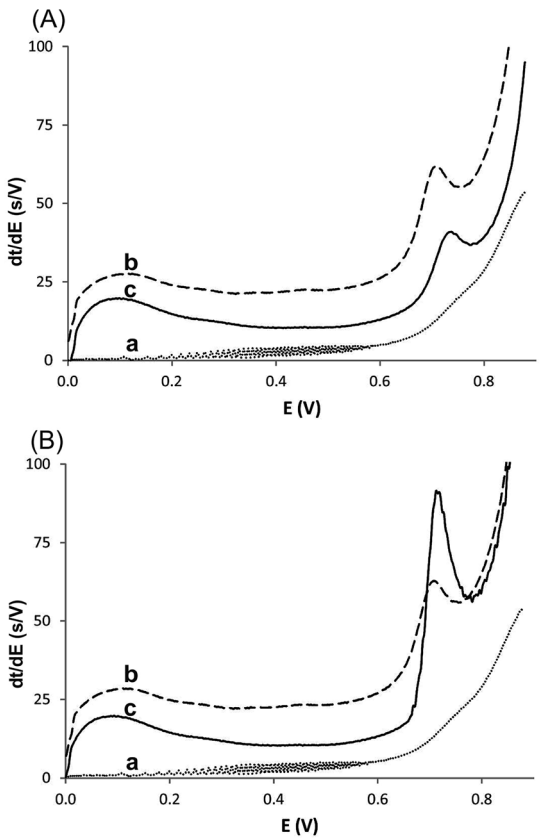

Fig. 2 CC-PSA results of Trp 10 (μM) analysis (A) immediately and (B) 5 min post incubation with Trp. These analyses were performed by (a) bare AuE, (b) MWCNT-AuE, and (c) Apt–MWCNT-AuE.

Fluorescent stains

Fig. S2 (see ESI†) shows the fluorescence staining of Trp Apt molecules attached to the surface of MWCNT-AuE *via* non-covalent interactions. Apt–MWCNT-AuE emitted orange fluorescence when stained with ethidium bromide (EtBr) and then irradiated with ultraviolet (254 nm); however, bare AuE and MWCNT-AuE were not stained with EtBr. These findings confirmed the successful deposition of Trp Apt molecules on the electrode surface.

Study of pH and supporting electrolyte effect on CC-PSA signals

The type and concentration of supporting electrolytes affect the CC-PSA background signals. We achieved the best responsiveness of the electrode using PBS (0.01 M) at pH 7 (for details, see Fig. S3, panels (A and B), see ESI†).

Effect of MWCNT content deposited on the electrodes

The amount of MWCNTs deposited on the surface had profound effects on the intensity of CC-PSA signals recorded. The increase in the content of MWCNTs (up to 12 μg) deposited showed a positive correlation with the CC-PSA signals recorded; however, signal saturation above 12 μg (for details, see Fig. S3, panel (C), see ESI†) was observed. This indicates that free sites were no longer available for the binding of MWCNTs to AuE. As a result, 12 μg of MWCNTs was considered as an optimal mass of deposition on AuE.

CC-PSA parameters optimization

Conditional potential (E_c), conditioning time (t_c) and stripping current (i_s) of CC-PSA experiments were optimized in this study. The results of optimizations are present in Fig. S4 (see ESI†). Briefly, the optimized conditions for CC-PSA experiments were $E_c = -0.2$ V, $t_c = 10$ s and $i_s = +5$ μA.

Effect of Apt content deposited on the electrode

Main parameters affecting the performance of the Apt–MWCNT-AuE were evaluated; for example, the optimal density of Apt deposited on the electrode surface was studied by CC-PSA. In the optimal density, the interference of Tyr in detection of Trp should be minimum. To this end, the designated amount of Apt in the range of 0.0–10.0 picomole was deposited on MWCNT-AuE and the CC-PSA signals were recorded in the presence of 10 μM Trp and 30 μM Tyr.

The maximum Trp and minimum Tyr signals were obtained from an electrode on which 5 picomole of Apt had been deposited (Fig. 3 (panels (A and B))); therefore, five picomole

was used as the optimal Apt content in experiments. At contents above 5 picomole, a decrease in the Trp CC-PSA signal was observed (Fig. 3, panel (B)), which might be due to the reduction of conductivity and saturation of the electrode surface.

Optimal time of Apt folding

To investigate whether incubation duration has an effect on the folding of Apt molecules and thus the performance of the Trp aptasensor, different incubation periods were tested. As shown in Fig. 3 (panels (C and D)), the CC-PSA signals increased until 5 min post-incubation and became stable, indicating that the majority of Apt molecules were completely folded by Trp molecules and that all sites for interactions were occupied.

After a 5 min incubation period, the CC-PSA signals of Tyr were not altered (Fig. 3, panel (D)), showing that Apt specifically targets Trp; therefore, a 5 min folding time was selected for the next experiments (Fig. 3, panels (C and D)).

Analytical application of the Trp aptasensor

Calibration graph and limit of detection (LOD). Under optimized conditions, the aptasensor responses increased linearly with increasing Trp concentrations in the ranges of 0.0001–10 and 10–300 μM. The LOD calculated from the calibration graph (Fig. 4) was found to be 64 pM (S/N = 3), which was lower than those reported in the literature (summarized in Table 1).

We carried out a set of electrochemical experiments using differential pulse voltammetry (DPV), amperometry, and CC-PSA techniques. The results showed that CC-PSA technique has significant superiority over other methods in terms of sensitivity, selectivity, reproducibility, and limit of detection (LOD) (Fig. S5, see ESI†).

Interference study

For real sample analyses, the effects of 18 different amino acids ascorbic acid (AAs), uric acid (UA), dopamine DA, glucose, and metal ions (*e.g.*, copper, zinc) on the measurement of Trp were evaluated in CC-PSA of the Trp aptasensor. Furthermore, the addition of various interfering species, especially Tyr, which is the main interfering substance usually found in biological samples along with Trp, did not result in any interference with the detection of Trp. Even a 25-

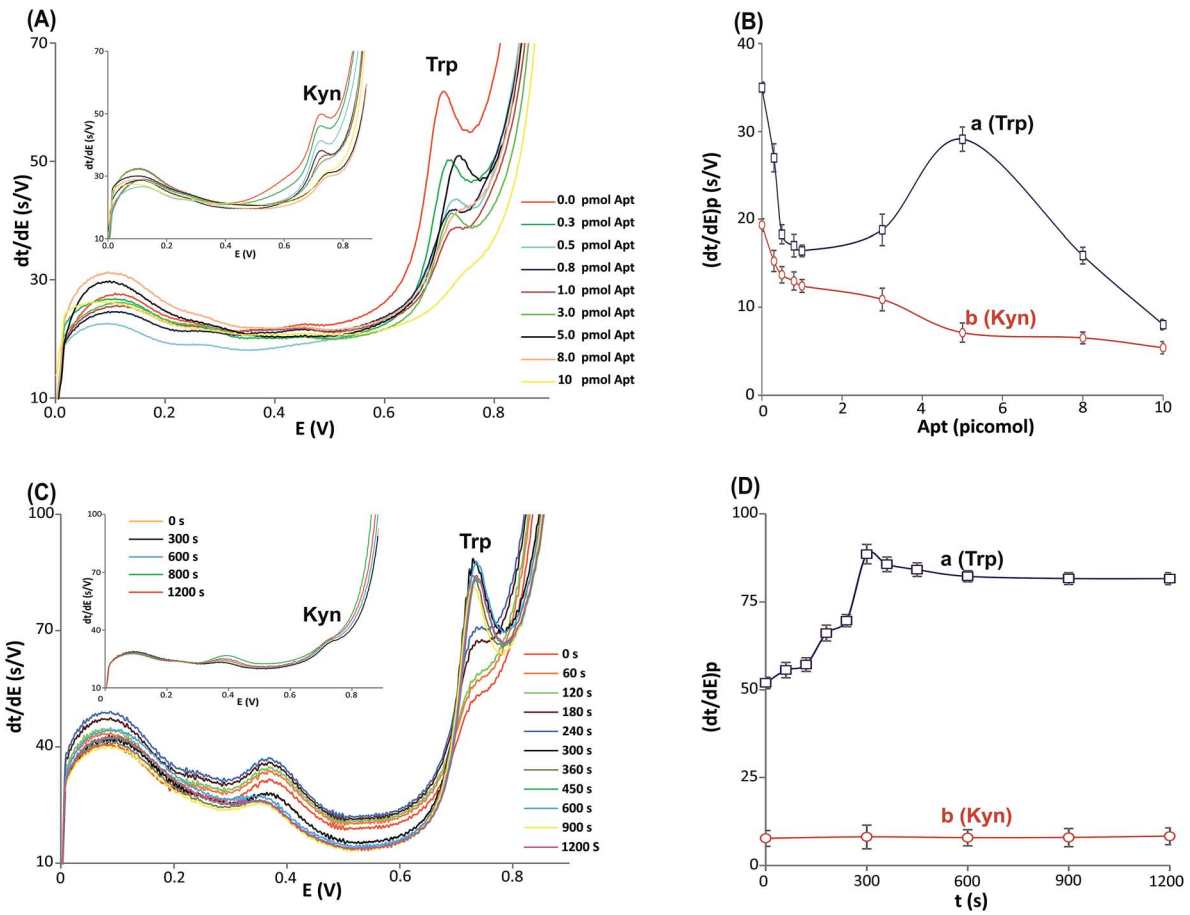

Fig. 3 (A) CC-PSA in the presence of 10 μM Trp and 30 μM Tyr (inset) using various amounts of Trp-specific Apt molecules. (B) The peak intensity of CC-PSA for Trp (curve (a)) and Tyr (curve (b)) with different amounts of Trp-specific Apt molecules. (C) CC-PSA in the presence of 10 μM Trp and 30 μM Tyr (inset) molecules incubated at different periods. (D) Peak intensity of CC-PSA for Trp (curve (a)) and Tyr (curve (b)) with different incubation periods. The error bars represent the standard deviation for three independent measurements.

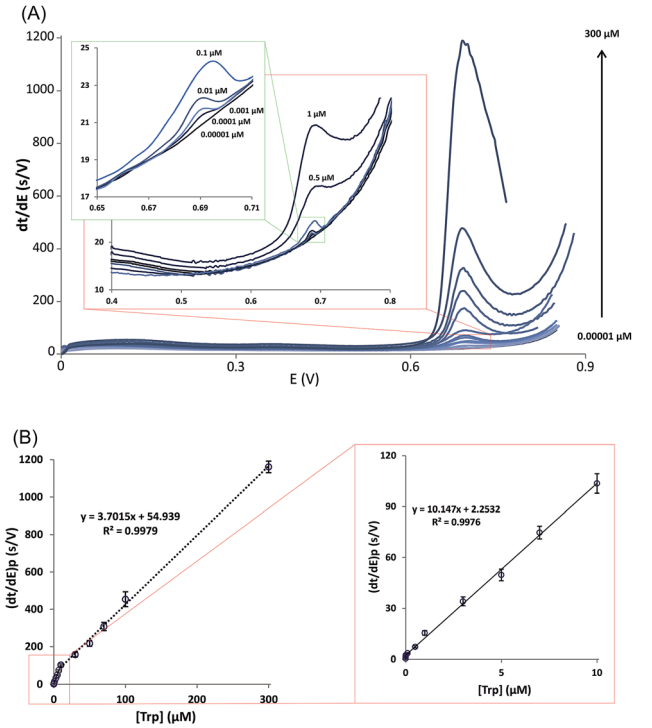

Fig. 4 (A) CC-PSA spectra for different concentrations of Trp (0.00001 to 300 μM in 0.01 M PBS buffer pH 7.0) recorded using the Apt–MWCNT-AuE (B) calibration curve of the analysis. The error bars represent the standard deviation for three independent measurements.

fold excess of Tyr produced a very faint signal (less than 1% of Trp signal), which can simply be ignored in Trp analysis (Fig. 5, panel (A)). In addition, the presence of UA, AA, DA, glucose and metal ions did not show any overlapping signals in the detection of Trp (Fig. 5, panel (A)). Furthermore, Trp-specific aptasensor were examined in Aminoven® 10% (a solution for infusion) using DPV, CV and CC-PSA (see Fig. S6 and Table S1, see ESI†). CC-PSA showed good accuracy and no interference of other AAs. In the voltammetry techniques, organic substances may give rise to background currents that can overlap the main peaks; however, CC-PSA technique is rather less sensitive to interference from electro-active substances present in complex media of biological samples. In addition, the duration of the stripping step in CC-PSA measurements is the physical parameter that can be measured with higher accuracy, precision, and resolution than the current, which is measured in voltammetry methods.

Analysis of Trp in real biological samples

The CC-PSA approach was used for the analysis of Trp in the diagnostic samples (Fig. 5, panel (B)). To this end, using the developed aptasensor and standard addition method, we analyzed the original content of Trp that exists in cow's milk and human blood serum, urine, and saliva samples. The engineered aptasensor could rapidly determine Trp concentrations in these samples with satisfactory accuracy and precision. Fig. 5 (panel (B)) and Table 2 show, respectively, the CC-PSA spectra and Trp concentration of milk, saliva, urine, and blood serum samples varying in the range of 76.21–174.38 μM. The analyses were also revalidated by HPLC (see Table 2 and Fig. S7, ESI†), showing good agreement.

Trp consumption pattern in different cancer cell lines

CC-PSA approach was used for the analysis of Trp in different cancer cell culture media. To this end, using the developed

Table 1 Comparison of the proposed method with previously published electrochemical methods used for detection of Trp[a]

Working electrode	Modifier	LOD (nM)	LDR (μM)	Techniques	Ref.
GCE	OD–AFMWCNT–ρ-AMT	0.54	0.025–0.3	DPV	39
ABPE	Schiff's base chitosan	2	0.6–2, 2–40, 40–100	AdSV	25
GCE	AgNPs–GO	2.0	0.01–800	DPV	40
GCE	HSA–MB–MWCNT	3.3	0.01–0.1	CV	40
ABPE	Schiff's base chitosan	2.0	0.06–2, 2–40, 40–100	AdSV	25
GCE	AuNPs–CNT	10	0.03–2.5	CA	24
GCE	MWCNT–FeNAZ–Chit	11	0.074–34	LSV	22
ITO	AuNP–MWCNT	25	0.5–90	SWV	23
PGE	ET	50	0.5–50	DPV	37
CPE	ET	9.8	0.04–0.49	AdSV	26
ABPE	GR	60	0.1–100	LSV	41
SGE	MWCNT	140	0.2–2.5	DPV	21
CPE	DMBQ–MWCNT	5000	0.1–700	SWV	42
Au	Apt–MWCNT	0.064	0.0001–10, 10–300	CC-PSA	This work

[a] ABPE: acetylene black paste electrode, AdSV: adsorptive stripping voltammetry, AFMWCNT: acid functionalized multiwalled carbon nanotubes, AgNPs: silver nanoparticles, AuNPs: gold nanoparticles, CA: chronoamperometry, Chit: chitosan, CNT: carbon nanotube, CPE: carbon paste electrode, DPV: differential pulse voltammetry, DMBQ: 2,6-dimethylbenzoquinone, ET: electrochemically treated, FeNAZ: iron ion-doped natrolite zeolite, GCE: glassy carbon electrode, GO: graphene oxide, GR: graphene, HSA: human serum albumin, ITO: indium tin oxide, LDR: linear detection range, LOD: limit of detection, LSV: linear sweep voltammetry MB: methylene blue, NSPPMA: nanocomposite silica perchloric acid poly(2-methyl aniline), OD: 1,8-octane diamine, ρ-AMT: 5-amino-2-mercapto-1,3,4-thiadiazole, PGE: pencil graphite electrode, SGE: sol–gel electrode, SWV: square wave voltammetry.

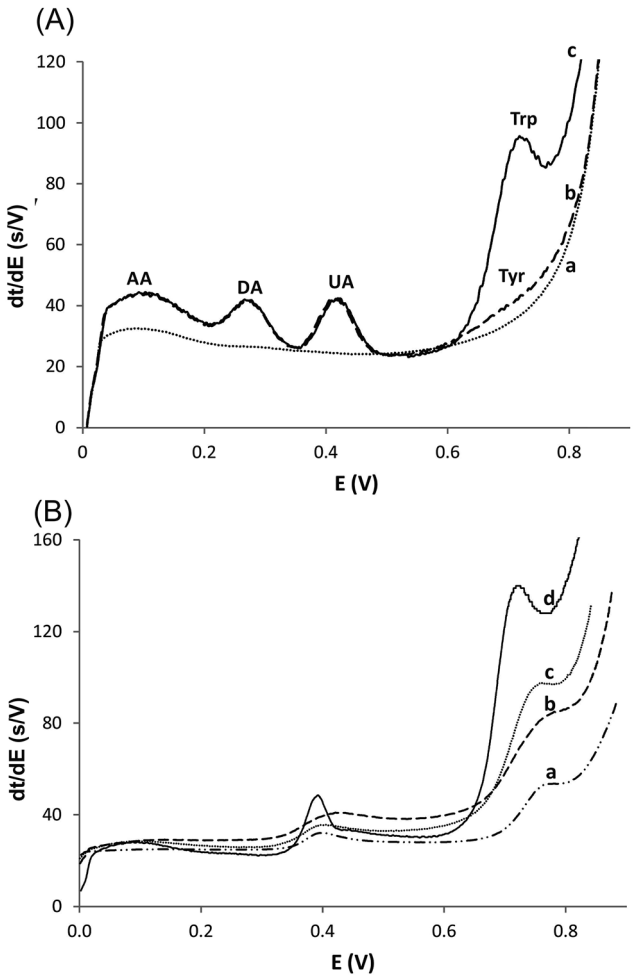

Fig. 5 (A) CC-PSA spectra of (a) PBS (0.01 M, pH 7.0), (b) interfering agents (*i.e.*, 100.0 μM AA, 50 μM DA, 100 μM UA, and 250 μM Tyr) in the absence of Trp, and (c) interfering agents in the presence of Trp (10 μM). (B) CC-PSA spectra of Trp in (a) blood serum, (b) saliva, (c) milk, and (d) urine samples.

aptasensor and standard addition method, we analysed the original rate of Trp consumption in human tumour cell lines including HepG2 (hepatocarcinoma), 1321NI (Astrocytoma), Calu-6 (lung carcinoma), NCI-H1299 (lung carcinoma), and HT29 (colorectal carcinoma). The engineered Apt–MWCNT-AuE (aptasensor) could determine the Trp concentrations in these samples with satisfactory accuracy and precision. Fig. 6 shows the concentration of Trp in the supernatants of the cancer cell lines cultured during three days. In addition, Table 3 shows the rate of Trp consumption by different cancer cell lines cultured during 3 days.

Metastatic cancer cells increase their Trp consumption by upregulating the enzymes[5,6] involved in the production of endogenous metabolites to evade the immune system and expand their invasiveness. The application of the aptasensor showed that HT29 cells, which have greater ability to migrate to different sites to form micrometastases, and HepG2 cells showing lower metastasis represented a higher and lower Trp consumption rate, respectively.

Reproducibility, stability and regeneration of the Trp aptasensor

Apt molecules on Apt–MWCNT-AuE could be regenerated successfully after each CC-PSA measurement, which is due to the oxidation and degradation of Trp molecules in folded Apt molecules. Hence, the aptasensor remained functional and serviceable for the next Trp analysis. Mean relative standard deviation (RSD) of this regeneration was found to be about 4.9% ± 0.9%, representing an appropriate reproducibility for 5 measurements (see Fig. S8, see ESI†). Moreover, reproducibility of the aptasensor fabrication process was investigated through an examination of Apt–MWCNT-AuE prepared independently. The inter-assay precision was found to be less than 5%. The stability of aptasensor was evaluated by the coefficient variation percentage (CV%) determination during 100 days. The engineered aptasensor was extremely stable during 48 days post-fabrication with a CV% less than 5%. After 48 days, CV% of measurements was less than 10%. All data on the reproducibility, stability and regeneration confirm the reliability of fabrication method for engineering this aptasensor.

Table 2 Analyses of Trp in different samples by the aptasensor and HPLC method[a]

Sample	HPLC [Trp], (μM)	Added [Trp], (μM)	Found by aptasensor [Trp], (μM)	*R* (%)
Serum (1)	5.63 ± 0.23	0	5.71 ± 0.74	101.4
Serum (2)	10.54 ± 0.18	20	30.11 ± 0.56	98.6
Serum (3)	7.66 ± 0.52	40	47.32 ± 0.79	99.3
Milk (1)	50.43 ± 0.61	0	51.10 ± 0.25	101.3
Milk (2)	62.64 ± 0.37	10	72.73 ± 0.17	100.1
Milk (3)	57.55 ± 0.44	30	86.63 ± 0.21	99.2
Urine (1)	160.03 ± 0.81	0	161.45 ± 0.91	100.9
Urine (2)	154.86 ± 0.64	5	158.96 ± 0.48	99.4
Urine (3)	171.73 ± 0.73	10	182.08 ± 0.57	100.2
Saliva (1)	32.17 ± 0.45	0	31.76 ± 0.23	98.7
Saliva (2)	20.03 ± 0.39	5	25.59 ± 0.75	102.2
Saliva (3)	27.25 ± 0.66	10	36.57 ± 0.47	98.2

[a] HPLC: high-performance liquid chromatography.

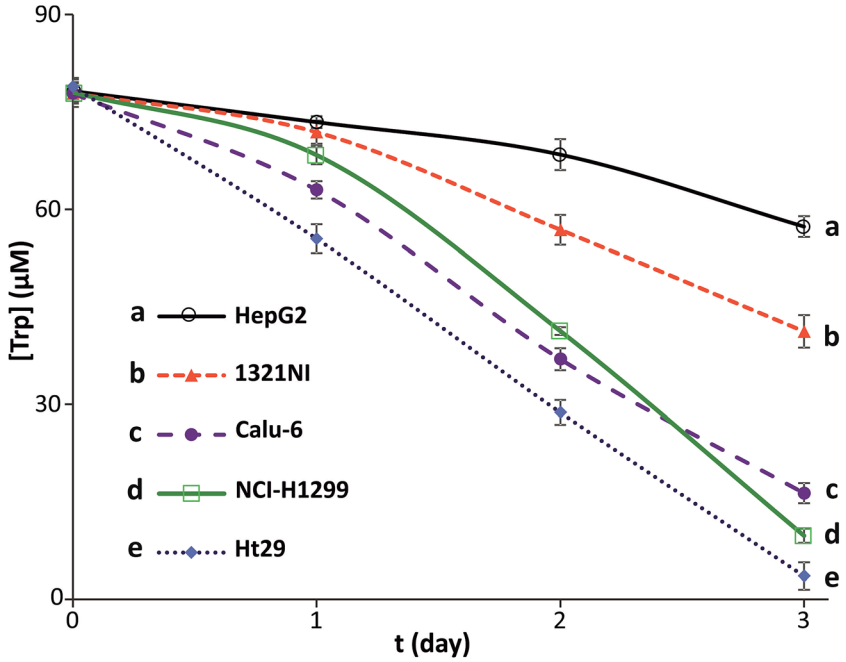

Fig. 6 Tryptophan concentration in the supernatants of HepG2 (a), 1321NI (b), Calu-6 (c), NCI-H1299 (d), and HT29 (e) cells plated under the conditions used for the cellular assay. The tryptophan concentration was measured by Apt–MWCNT-AuE.

Table 3 Analyses of Trp consumption in different cancer cell culture media samples by CC-PSA at Apt–MWCNT-AuE

Cell lines	Day	Cell count	[Trp] (μM)	Trp consumption (μM/24 h/10^6 cell)
HepG2	0	100 000 ± 92	78.2 ± 1.2	27.86 ± 1.53
	1	172 727 ± 58	73.5 ± 0.9	
	2	298 347 ± 169	68.4 ± 2.4	
	3	515 327 ± 207	57.3 ± 1.6	
1321NI	0	100 000 ± 73	77.9 ± 2.1	34.82 ± 2.18
	1	196 000 ± 112	71.9 ± 1.8	
	2	384 160 ± 187	61.8 ± 2.3	
	3	752 954 ± 157	45.2 ± 2.5	
Calu-6	0	100 000 ± 86	77.8 ± 1.6	57.49 ± 2.54
	1	180 000 ± 142	69.5 ± 1.4	
	2	324 000 ± 115	51.7 ± 1.7	
	3	583 200 ± 263	33.2 ± 1.6	
NCI-H1299	0	100 000 ± 101	78.0 ± 1.5	65.07 ± 2.85
	1	209 091 ± 223	63.4 ± 1.4	
	2	437 190 ± 298	41.3 ± 0.6	
	3	914 125 ± 396	19.7 ± 1.1	
HT29	0	100 000 ± 68	78.9 ± 1.3	91.95 ± 1.88
	1	223 077 ± 126	51.5 ± 2.2	
	2	497 633 ± 179	22.8 ± 1.1	
	3	1 110 105 ± 342	1.7 ± 0.1	

Conclusion

L-Tryptophan is an essential amino acid that plays unique actions in human biologic systems, in which the key intermediates are produced in metabolic pathways. Trp determination by a rapid, highly selective, and ultra-sensitive technique such as using biosensors can be of assistance in numerous clinical studies, particularly for the treatment and early diagnosis of neurological disorders and malignancies. Considering the importance of sensors/biosensors in the detection of clinically important molecular markers, we developed an aptasensor based on the non-covalent attachment of MWCNT and Trp Apt molecules, which could detect ultra-small quantities of Trp in human diagnostic samples. The interference of tyrosine that can significantly affect the accuracy, sensitivity, and selectivity of Trp determination was reduced considerably by applying Apt

molecules and CC-PSA technique. The engineered aptasensor could provide highly improved LOD and broad LDR. Furthermore, it was evident that non-covalent attachment-based aptasensor not only could produce accurate and reproducible results but could also improve the LOD and LDR values significantly. Overall, based on the great potential of this Trp aptasensor, we suggest it as a robust bio-sensing tool for the quantitative detection of Trp whose fast and accurate detection is of great interest in the study of several neurological/psychological disorders and malignancies.

Acknowledgements

Authors would like to acknowledge the technical support provided by the Faculty of Chemistry at University of Tabriz and the financial and technical supports provided by the Research Centre for Pharmaceutical Nanotechnology (RCPN) at Tabriz University of Medical Sciences.

Notes and references

1 J. R. Moffett and M. A. A. Namboodiri, *Immunol. Cell Biol.*, 2003, **81**, 247–265.
2 J. P. Roiser, J. Levy, S. J. Fromm, H. Wang, G. Hasler, B. J. Sahakian and W. C. Drevets, *Neuropsychopharmacology*, 2007, **33**, 1992–2006.
3 L. Vecsei, L. Szalardy, F. Fulop and J. Toldi, *Nat. Rev. Drug Discovery*, 2013, **12**, 64–82.
4 I. Arnulf, P. Quintin, J.-C. Alvarez, L. Vigil, Y. Touitou, A.-S. Lebre, A. Bellenger, O. Varoquaux, J.-P. Derenne, J.-F. Allilaire, C. Benkelfat and M. Leboyer, *Neuropsychopharmacology*, 2002, **27**, 843–851.
5 H. K. Koblish, M. J. Hansbury, K. J. Bowman, G. Yang, C. L. Neilan, P. J. Haley, T. C. Burn, P. Waeltz, R. B. Sparks, E. W. Yue, A. P. Combs, P. A. Scherle, K. Vaddi and J. S. Fridman, *Mol. Cancer Ther.*, 2010, **9**, 489–498.
6 P. H. Tan and A. K. Bharath, *Expert Opin. Ther. Targets*, 2009, **13**, 987–1012.
7 I. A. Murray, A. D. Patterson and G. H. Perdew, *Nat. Rev. Cancer*, 2014, **14**, 801–814.
8 C. A. Opitz, U. M. Litzenburger, F. Sahm, M. Ott, I. Tritschler, S. Trump, T. Schumacher, L. Jestaedt, D. Schrenk, M. Weller, M. Jugold, G. J. Guillemin, C. L. Miller, C. Lutz, B. Radlwimmer, I. Lehmann, A. von Deimling, W. Wick and M. Platten, *Nature*, 2011, **478**, 197–203.
9 G. C. Prendergast, *Oncogene*, 2008, **27**, 3889–3900.
10 E. W. Yue, B. Douty, B. Wayland, M. Bower, X. Liu, L. Leffet, Q. Wang, K. J. Bowman, M. J. Hansbury, C. Liu, M. Wei, Y. Li, R. Wynn, T. C. Burn, H. K. Koblish, J. S. Fridman, B. Metcalf, P. A. Scherle and A. P. Combs, *J. Med. Chem.*, 2009, **52**, 7364–7367.
11 G. C. Prendergast, *Nature*, 2011, **478**, 192–194.
12 M. Sano, V. Ferchaud-Roucher, C. Nael, A. Aguesse, G. Poupeau, B. Castellano and D. Darmaun, *J. Mass Spectrom.*, 2014, **49**, 128–135.
13 J. Zhao, *Biomed. Chromatogr.*, 2015, **29**, 410–415.
14 S. A. Çevikkalp, G. B. Löker, M. Yaman and B. Amoutzopoulos, *Food Chem.*, 2016, **193**, 26–29.
15 B. J. Sanghavi, G. Hirsch, S. P. Karna and A. K. Srivastava, *Anal. Chim. Acta*, 2012, **735**, 37–45.
16 X. Zhang, Y. He and M. Ding, *J. Chromatogr. B: Anal. Technol. Biomed. Life Sci.*, 2009, **877**, 1678–1682.
17 M. A. Malone, H. Zuo, S. M. Lunte and M. R. Smyth, *J. Chromatogr. A*, 1995, **700**, 73–80.
18 J. Lehmann, *Scand. J. Clin. Lab. Invest.*, 1971, **28**, 49–55.
19 I. N. Mefford and J. D. Barchas, *J. Chromatogr. B: Biomed. Sci. Appl.*, 1980, **181**, 187–193.
20 G. N. Chen, R. E. Lin, Z. F. Zhao, J. P. Duan and L. Zhang, *Anal. Chim. Acta*, 1997, **341**, 251–256.
21 M. R. Majidi, A. Salimi and E. Alipour, *Chin. J. Chem.*, 2013, **60**, 1473–1478.
22 M. Noroozifar, M. Khorasani-Motlagh, R. Akbari and M. Bemanadi Parizi, *Biosens. Bioelectron.*, 2011, **28**, 56–63.
23 R. N. Goyal, S. Bishnoi, H. Chasta, M. A. Aziz and M. Oyama, *Talanta*, 2011, **85**, 2626–2631.
24 Y. Guo, S. Guo, Y. Fang and S. Dong, *Electrochim. Acta*, 2010, **55**, 3927–3931.
25 P. Deng, J. Fei and Y. Feng, *Analyst*, 2011, **136**, 5211–5217.
26 H. Wang, H. Cui, A. Zhang and R. Liu, *Anal. Commun.*, 1996, **33**, 275–277.
27 N. E. Zoulis, D. P. Nikolelis and C. E. Efstathiou, *Analyst*, 1990, **115**, 291–295.
28 A. D. Ellington and J. W. Szostak, *Nature*, 1990, **346**, 818–822.
29 M. Ebrahimi, H. Hamzeiy, J. Barar, A. Barzegari and Y. Omidi, *Sens. Lett.*, 2013, **11**, 566–570.
30 T. Bing, X. Liu, X. Cheng, Z. Cao and D. Shangguan, *Biosens. Bioelectron.*, 2010, **25**, 1487–1492.
31 T.-Y. Liu, F.-Y. Yeh, I.-H. Tseng, C.-W. Yang, L.-C. Lu and C.-S. Lin, *Biosens. Bioelectron.*, 2014, **61**, 336–343.
32 Y. Lian, F. He, H. Wang and F. Tong, *Biosens. Bioelectron.*, 2014, **65**, 314–319.
33 I. Majerfeld and M. Yarus, *Nucleic Acids Res.*, 2005, **33**, 5482–5493.
34 C. Bearcroft, M. Farthing and D. Perrett, *Biomed. Chromatogr.*, 1995, **9**, 23–27.
35 H. Angerstein-Kozlowska, B. Conway, A. Hamelin and L. Stoicoviciu, *Electrochim. Acta*, 1986, **31**, 1051–1061.
36 X. Cai, G. Rivas, P. A. Farias, H. Shiraishi, J. Wang and E. Palecek, *Electroanalysis*, 1996, **8**, 753–758.
37 A. Özcan and Y. Şahin, *Biosens. Bioelectron.*, 2012, **31**, 26–31.
38 N. Nguyen, M. Z. Wrona and G. Dryhurst, *J. Electroanal. Chem. Interfacial Electrochem.*, 1986, **199**, 101–126.
39 K. Rajalakshmi and S. A. John, *J. Electroanal. Chem.*, 2014, **734**, 31–37.
40 J. Li, D. Kuang, Y. Feng, F. Zhang, Z. Xu, M. Liu and D. Wang, *Biosens. Bioelectron.*, 2013, **42**, 198–206.
41 P. Deng, Z. Xu and Y. Feng, *Mater. Sci. Eng., C*, 2014, **35**, 54–60.
42 M. Asnaashariisfahani, H. Karimi-maleh, H. Ahmar, A. A. Ensafi, A. R. Fakhari, M. A. Khalilzadeh and F. Karimi, *Anal. Methods*, 2012, **4**, 3275–3282.
43 S. Tanaka, M. Machino, S. Akita, Y. Yokote and H. Sakagami, *In Vivo*, 2010, **24**, 853–856.